Optical Fiber Technology 72 (2022) 102994

Contents lists available at ScienceDirect

Optical Fiber Technology

journal homepage: www.elsevier.com/locate/yofte

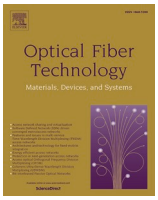

Fibre laser system with wavelength tuning in extended telecom range

D. Stoliarov [a,*], A. Koviarov [a], D. Korobko [b], D. Galiakhmetova [a], E. Rafailov [a]

[a] Aston Institute of Photonic Technologies, Aston University, Birmingham B4 7ET, UK
[b] Ulyanovsk State University, 42 Leo Tolstoy Street, Ulyanovsk 432017, Russia

ARTICLE INFO

Keywords:
Fibre lasers
Optical soliton
Raman scattering
Self-frequency shift
Self-phase modulation
State of polarisation
Isotropy
Large mode area
Photonic crystalfibres
Nonlinearity

ABSTRACT

We report on a laser system on the base of a fibre telecom source, a chirped pulse amplification system, and low-birefringence large mode area photonic crystal fibre (LMA PCF) generating ~ 100 fs pulses with the energy ~ 10 nJ in the 1600–1700 nm wavelength range. The characteristics of the output spectrum corresponding to Raman solitons are studied for different polarisations of the pump pulse at the input of the PCF. We have shown that the wavelength of the output spectrum maximum can be tuned in the whole long (L) and ultra-long (U) telecom bands by adjusting the polarisation state of the pump pulse while the output power is constant.

1. Introduction

In addition to the well-known problem related to the growing demands in telecom fibre optical data transmission lines with extended bandwidth [1,2] in recent years the researchers developed an interest in the pulsed lasers of 1600–1700 nm spectral region in a number of biomedical applications [3]. This wavelength area is located in the third optical window, and defines the spectral region where the light has minimum scattering losses and a maximum depth of penetration in tissue, so these sources are in high demand in the development of multiphoton imaging system [4,5]. An extremely attractive property of the multiphoton imaging laser source is the possibility of broad wavelength tuning [5]. This property contributes deeper penetration length and better optical images of the abnormalities hidden behind different types of tissues [6].

One of the approaches to fibre lasers developing in the wavelength region of 1600–1700 nm is the usage of Bismuth or Thulium doped fibres with luminescence window in this spectral range [7–9]. Nevertheless, despite the unique optical properties of these fibres and significant achievements in their applications, their fundamental limitations should be noted. The lasing emission band of the Tm-doped fibre lasers is shifted to the region beyond 1700 nm, but the Bi-doped fibres in turn suffer from a relatively low gain and, at the same time, sufficiently high absorption negatively affecting the stability of mode-locking. As a result, we choose another approach based on the Er-doped fibre mode-locked seed source of telecom range ($\lambda \approx 1550$ nm). The output ultrashort pulse then propagates in nonlinear optical fibre with anomalous dispersion undergoing the Raman shift (also known as self-soliton frequency shifting (SSFS)) to the longer wavelengths [10–13]. The benefits of this approach are not only advanced technologies of telecom mode-locked fibre lasers, but also the possibility of simple pulse central wavelength tuning due to varying value of the Raman shift. The parameters of the output fibre are particularly restricted by the requirements of multiphoton imaging systems, which declare the minimum pulse energy of about 1 nJ [14]. The relatively high nonlinearity of standard single-mode fibres prevents the achievement of energies in nJ range leading to mandatory application of the output fibre with low nonlinearity, for example, LMA PCF with a mode area up to 500 μm^2 or more. The "hollow" core PCF fibres have even lower nonlinearity but the LMA PCF are characterised by lower bending losses and significantly greater wavelength tuning capabilities [15].

The well-known way to tune the output laser central wavelength with SSFS is to control the peak power of the laser pulse at the input of the PCF. The dependence of the Raman soliton energy on the value of the wavelength shift is the serious drawback of this method particularly for multiphoton imaging applications. Another approach in SSFS wavelength tuning relates to the chirp-based control technique, but it suffers from the same disadvantages [16,17]. An alternative way utilising the

* Corresponding author.
E-mail address: d.stoliarov@aston.ac.uk (D. Stoliarov).

https://doi.org/10.1016/j.yofte.2022.102994
Received 25 March 2022; Received in revised form 28 June 2022; Accepted 16 July 2022
Available online 30 July 2022

change of the initial pulse polarisation state typically relates to the output fibre with high birefringence [18]. Polarisation rotation of the initial linearly polarised pulse at the input of the anisotropic fibre can induce the elliptical polarisation of the propagating pulse leading to the different spectral shift for each of the polarisation component. This method has been successfully applied in supercontinuum generation [19,20]. Yu Du et al. with the technique of combining power and polarisation control in a polarisation-maintaining LMA fibre showed that the power of the pulse polarisation components could be individually adjusted [21]. In [22] the authors investigated the central wavelength tuning of the Raman soliton by varying the linear polarisation of the initial pulse at the input of a high birefringent PCF numerically. The experimental investigation of SSFS polarisation tuning in fibres with low birefringent is rather a difficult task because of the strict twisting control and minimisation of external impacts are required. Some experimental results on soliton Raman shift in the low birefringent fibres pumping by linearly polarised pulses one can find in [23]. Recent studies of the SSFS evolution in an isotropic PC-rod has shown that wavelength-shifted, elliptically-polarised solitons can be generated by the elliptically-polarised input pulse [24]. The authors demonstrated that in order to achieve necessary wavelength of the SSFS, a certain energy of the input pulse depending on its polarisation state is required. The results show that the required input pulse energy is the lowest for a linearly polarised pump pulse, and is the highest for a circularly polarised pulse.

In this paper, we consider the polarisation tuning of the wavelength of Raman soliton with fixed output power in a commercially accessible LMA PCF fibre with low birefringence. The evolution of the pulse propagating in the LMA PCF is studied experimentally through investigation of the SSFS and output polarisation depending on the polarisation state of the initial pulse with fixed energy. We have also shown the advantage of the SSFS polarisation tuning over the power-based Raman shift control in the LMA PCF. It is established that the correct adjustment of the input pulse polarisation can lead to the wavelength shift of the output Raman soliton in the targeted range of 1600–1700 nm while maintaining its energy. The output pulse with a duration of less than 100 fs and an energy of up to 10 nJ is quite enough for operation in deep tissue multiphoton imaging system [25].

2. Experimental setup

Our experimental setup is schematically shown in Fig. 1. The seed laser is an all-PM fibre oscillator mode-locked with a nonlinear amplifying loop mirror. The oscillator output average power of 1.62 mW corresponding to the single pulse energy of 0.15 nJ is achieved at the measured pulse repetition rate of 10.9 MHz. The preamplifier on the base of heavily Er-doped single-mode fibre provides the 15 mW average power. After that the pulse stretched from 2.3 ps to 40.6 ps in the FBG stretcher with a total dispersion of −4.4 ps/nm. Before the power amplifier, the isolator with a blocked fast axis of polarisation sets the linear polarisation of the pulse. Finally, the radiation is amplified in the PM double-clad Er/Yb co-doped fibre with a 10 μm core diameter pumped by two high-power 980 nm laser diodes (LD). The maximal output power of the system of 1.2 W is achieved at the pump power of 7 W. The pulse from the output of the power amplifier with duration of about 35 ps is compressed with a free space compression system made of a pair of diffraction gratings (1000 lines per mm, the Littrow angle of 49.9°). The linear polarisation ensures minimal radiation losses on each grating (less than 5 %). Adjusting the distance between the gratings to 160 mm (corresponding to the dispersion of 3.7 ps/nm) we reach the compressed pulse duration of 660 fs at the average output power of 1 W. The spectrum and autocorrelation trace of the compressed pulse recorded by the optical spectrum analyser Ando AQ-6315E and autocorrelator Femtochrome FL103XL respectively are shown in Fig. 2 (a, b). The autocorrelation trace contains a noticeable pedestal (Fig. 2 b). Gaussian fitting confirms that 72 % of the pulse energy is contained within the main peak, which indicates acceptable compression quality. The compressed pulse duration is weakly dependent on the output power. As will be seen further, an average output power of about 350 mW corresponding to the amplifier output pulse energy of ~ 32 nJ and peak soliton power of about 37 kW is sufficient to shift the Raman soliton to the wavelength of 1700 nm.

After compression, the pulse is launched into the LMA PCF through a special density filter. Input power was adjusted through that while other pulse parameters were maintained. The commercially available PCF-LMA-20 (NKT) has the following parameters: the nonlinearity is $\gamma = 4 \times 10^{-4}$ /W/m; the dispersion coefficients are $\beta_2 = -3.7 \times 10^{-26}$ s^2/m, $\beta_3 = 1.5 \times 10^{-40}$ s^3/m, $\beta_4 = -3.1 \times 10^{-55}$ s^4/m at 1550 nm. The coupling efficiency to the PCF-LMA fibre is about 70 %. Fig. 2 (c) shows the output spectrum recorded after propagation through the 1 m LMA PCF the 660 fs pulse with the peak power of 24 kW (corresponding to the average output power of the amplifier of 230 mW). In this experiment, the pulse polarisation is controlled at the amplifier output only and turns to be slightly elliptical at the PCF input. Comparing the Fig (c) with the (a) one can note the higher-order soliton evolution dynamics of spectral broadening (also known as "soliton fission") including the generation of Raman soliton [10]. Its spectrum is well observed around the 1675 nm.

To demonstrate the low-birefringence of the PCF (B = 10^{-7}), we investigate the effect of the polarisation rotation on the Raman soliton shift experimentally. Fig. 3 shows the spectra of the Raman shifted soliton for different linear polarisation states of the launched pulse. The linear polarisation of the input pulse is rotated by zero-order half-wave plate. One can see that the change of the input linear polarisation has nearly no effect on the Raman soliton spectrum confirming the low birefringence of the PCF. Transforming the linear polarisation into the circular by the zero-order quarter-wave plate one can observe the similar results, but with the decreased value of the Raman shift. In

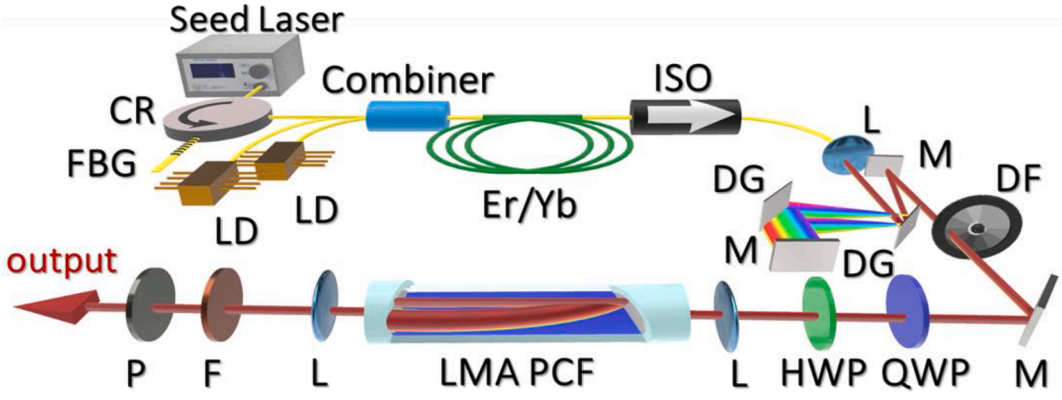

Fig. 1. Experimental setup. CR – circulator, LD – laser diodes, L – aspherical lenses, FBG – fibre Bragg-grating stretcher, ISO – isolator, DG – dispersion gratings, M – dielectric mirror, QWP – quarter-wave plate, HWP – half-wave plate, DF – density filter, F – long-pass filter, P – polariser.

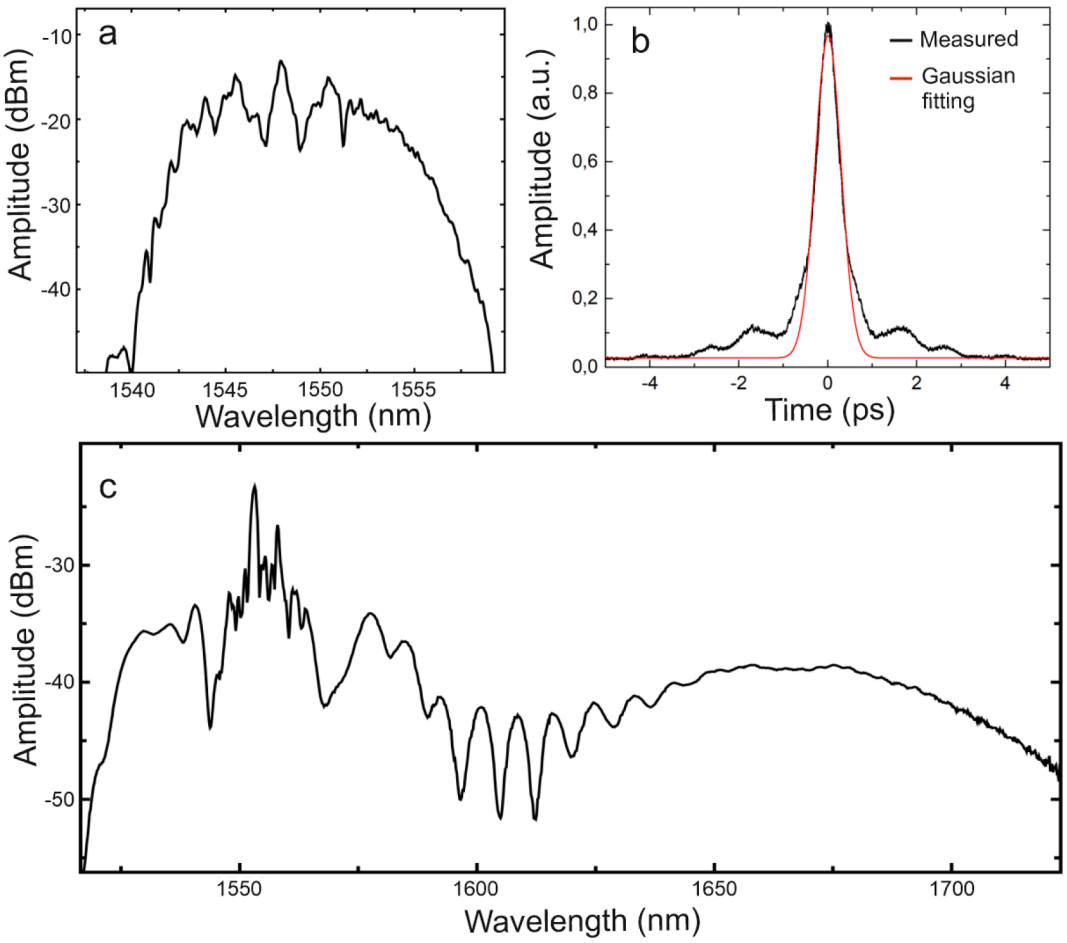

Fig. 2. (a) Spectrum and (b) autocorrelation trace of the compressed pulse corresponding to the average output power of amplifier ~ 1 W, (c) spectrum at the output of LMA PCF with launched 660 fs pulse with the peak power of 24 kW.

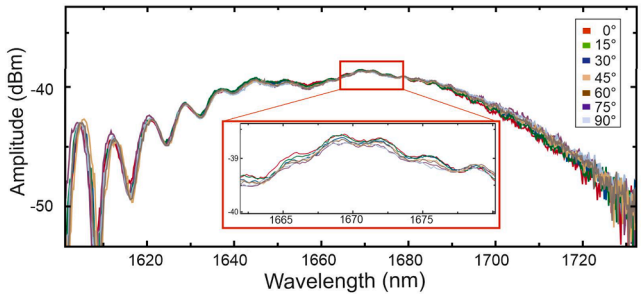

Fig. 3. Output spectra for various linear polarisation angles θ of the pulse measured at the input of the LMA PCF.

particular, in order to achieve the shift to the 1675 nm wavelength the average power of the circularly polarised radiation at the input of the PCF should be raised up to 290 mW corresponding to the pulse peak power of about 31 kW.

3. Raman shift tuning

In this section, we describe the different methods of the Raman soliton wavelength tuning. Figs. 4 and 5 demonstrate the results of the power-based Raman shift tuning for linear and circular polarisations fixed at the input of the PCF, respectively. After compression, the pulse is launched into the LMA PCF through a special density filter allowing to adjust the input power while other pulse parameters are maintained.

It is well known, that there are several stages of the *N*-soliton pulse propagation in optical nonlinear fibre. At the first stage, the initial pulse is compressed due to cooperation of self-phase modulation and anomalous dispersion, and its spectrum is strongly broadened. In the next stage, the fundamental solitons are sequentially detached off the main pulse, shifting to the long-wavelength part of the spectrum due to Raman scattering [26]. In our case, we isolate the long-wavelength part of the output pulse spectrum corresponding to Raman solitons by a special 1600 nm long pass filter. The soliton order of the pulse launched at the PCF input for an average power of 230 mW is $N = 6$. After the propagation through the PCF in the spectral region with $\lambda > 1600$ there are one or two Raman solitons depending on the power of the input pulse. In the first and second lines of Figs. 4, 5 one can see the filtered output spectrum, corresponding to the first detached Raman soliton. In the bottom lines, the appearance of the second detached soliton is noticeable, in particular one can see the spectrum modulation that could be explained by the interference between the first and the second Raman solitons. The higher the input pulse power, the earlier the separation of the first Raman soliton occurs. During the propagation, the Raman soliton is temporally compressed and its spectrum broadens. One can see this sequentially comparing the spectra and autocorrelation traces corresponding to increasing power of the input pulse. The linear polarisation of the input pulse provides the first Raman soliton on 1675 nm with the energy estimated as 8.5 nJ while its peak power is about 27 kW. In case of the circularly polarised initial pulse, the peak power of the soliton decreases due to the polarisation energy separation. As a result, the soliton with the same energy undergoes a smaller frequency shift. Thus, to achieve the Raman soliton at the wavelength of 1675 nm, the

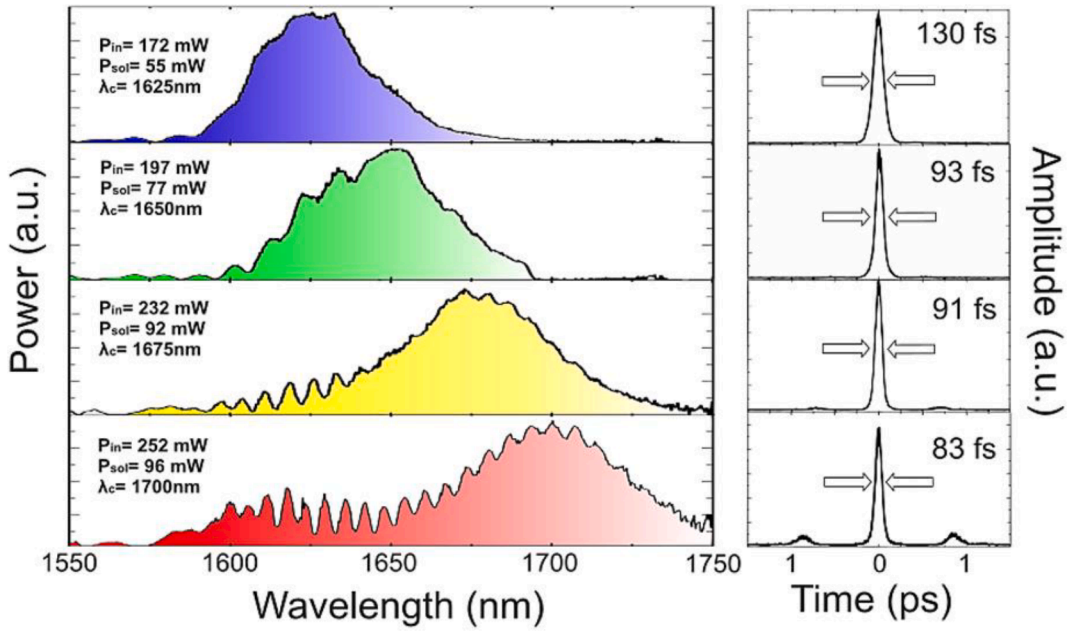

Fig. 4. Spectra and autocorrelation traces of the Raman shifted soliton in the PCF for different powers of the input pulse with fixed linear polarisation. P_{in} – the average power at the input of the PCF; P_{sol} – the average power at the output of the PCF after the 1600 nm long-pass filter; λ_c – the central wavelength of Raman shifted soliton.

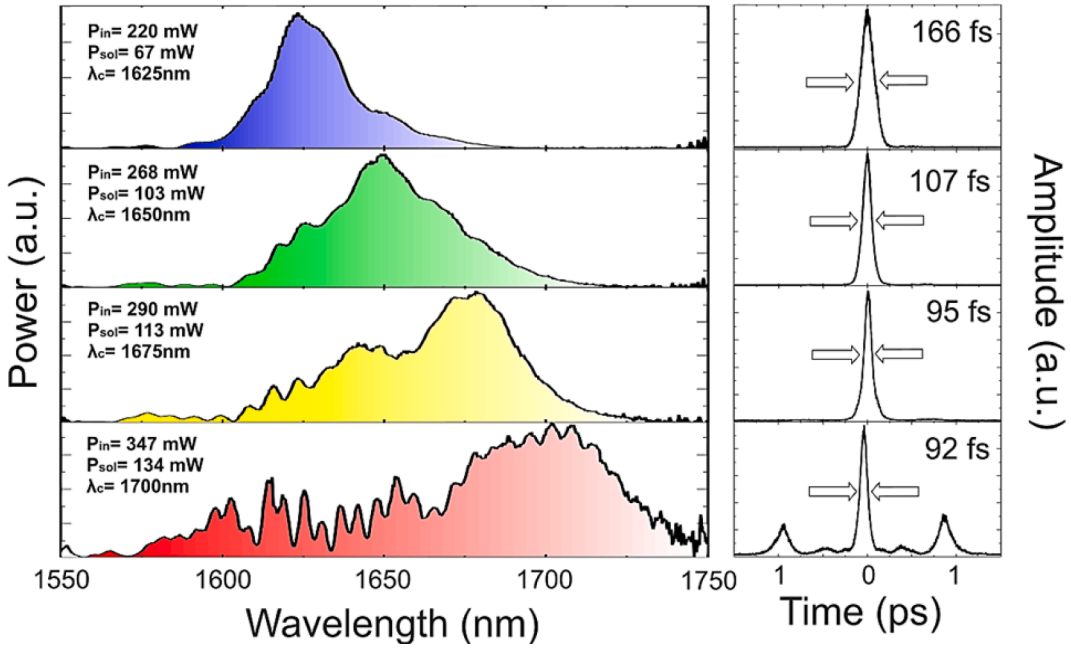

Fig. 5. Spectra and autocorrelation traces of the Raman shifted soliton in the PCF for different powers of the input pulse with fixed circular polarisation. P_{in} – the average power at the input of the PCF; P_{sol} – the average power at the output of the PCF after the 1600 nm long-pass filter; λ_c – the wavelength of the spectrum maximum corresponding to the central wavelength of the first Raman shifted soliton.

initial pulse peak power must be increased leading to increase of the Raman soliton energy up to 10.4 nJ. Finally, we should note that in order to get the long-wavelength limit of the targeted range the input average power values about 250 mW or 350 mW are quite enough for linear and circular input pulse polarisation states, respectively.

Next, we consider the possibility of the Raman shift tuning by the control of the polarisation of the pulse launched into the PCF. This method implies the constant power of the input radiation that we fixed at the level of 252 mW. By rotating the QWP, the polarisation of the input pulse can be continuously transformed from circular to linear through a series of intermediate elliptically polarised states. To control the polarisation, we used the fast polarimeter Novoptel PM1000. The polariser installed at the output of the PCF after the long-pass filter allows us to analyse the polarisation of the output radiation component-wise. Fig. 6 shows the experimental results of the Raman shift tuning by adjusting the polarisation of the input pulse.

The spectrum of the output Raman soliton (red highlighted area) is the sum of two polarisation components: the s-component (blue area), and the p-component (green area), which are measured independently. The average output powers of s- and p- components and the central

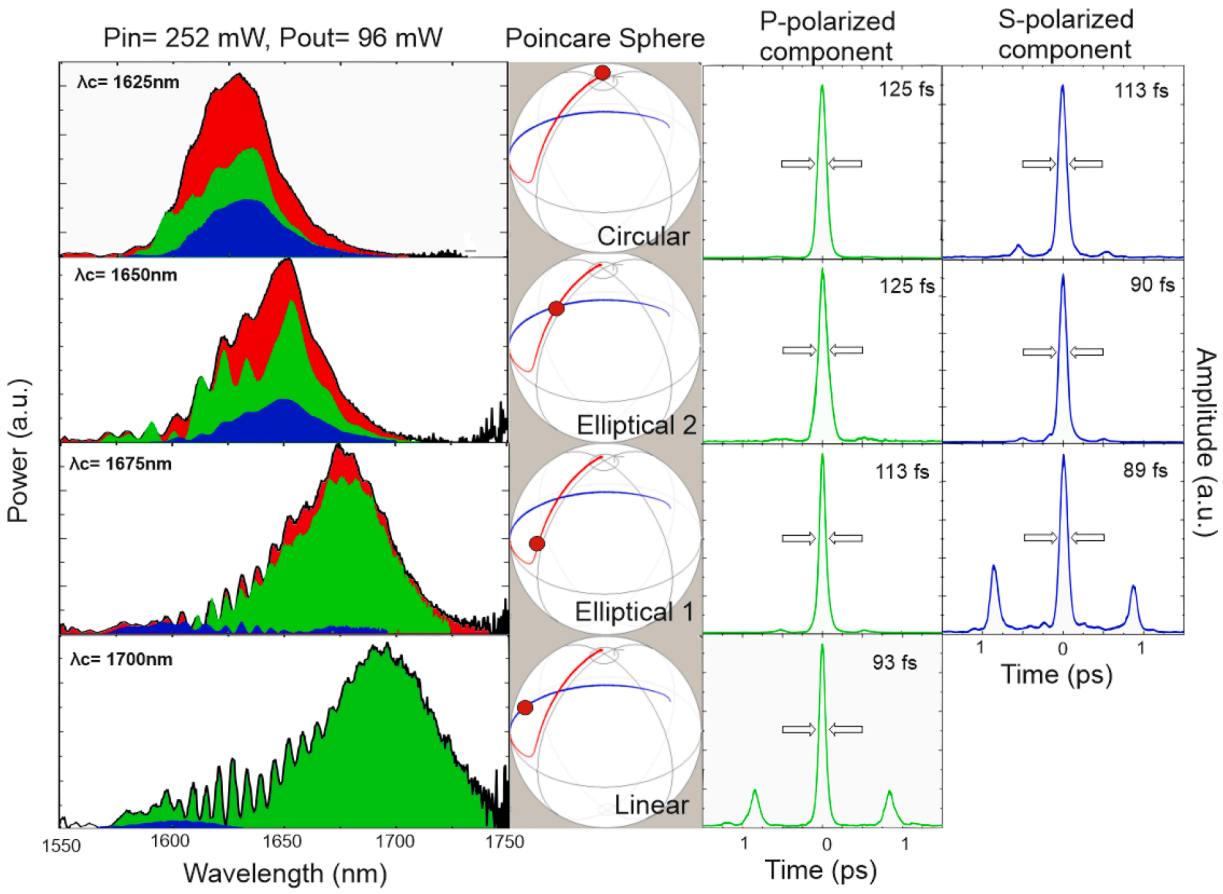

Fig. 6. Spectra and autocorrelation traces of the Raman shifted soliton for different polarisations of the input pulse. P_{in} is the average power at the input of the PCF; P_{out} is the average power at the output of PCF after the 1600 nm long-pass filter; λ_c - is the wavelength of the spectrum maximum corresponding to the central wavelength of the first Raman shifted soliton.

wavelength λ_c of the Raman soliton for different polarisations of the input pulse are listed in the Table 1. These values correspond to the average power at the PCF input Pin = 252 mW and the total output power after the long-pass filter Pout = 96 mW. The colored dot on the Poincaré sphere corresponds to the polarisation state of the pulse at the input to the PCF. We will discuss the experimental results, starting with the linear polarisation of the input pulse (bottom line in Fig. 6). Despite the low PCF birefringence, a small s-polarised power orthogonal to the polarisation state of the initial pulse is detected at the PCF output. This small power is located in the spectral range associated with the second Raman soliton detached off the original pulse. The low output power prevents obtaining the autocorrelation of the s-polarised pulse. However, the main power (more than 97.5 %) of the output signal refers to the p-polarisation component, while the main spectral maximum associated with the first Raman soliton is located at the wavelength of 1700 nm. In this case, the soliton duration is minimal and it is measured as 93 fs. The second Raman soliton observed in the autocorrelation trace also manifests itself in spectral modulations similar to Figs. 4-5.

Table 1
The average output powers of s- and p- components and the central wavelength λ_c of the Raman soliton for different states of polarisations (SOP) of the input pulse. $P_{s\ out}$ is the power of the s-polarisation component at the output of the PCF after 1600 nm long-pass filter and polariser; $P_{p\ out}$ is the power of the p-polarisation component at the output of LMA PCF and after 1600 nm long-pass filter and polariser;

SOP	$P_{s\ out}$, mW	$P_{p\ out}$, mW	λ_c, nm
Linear	2	94	1700
Elliptical 1	7	91	1675
Elliptical 2	20	76	1650
Circular	35	31	1625

When the polarisation state of the input pulse turns to be elliptical, the power of the output s-component increases but the p-component power decreases, while the total output power passed through the long-pass filter remains the same. The decrease of the p-component with maximum peak power leads to decrease of the Raman shift in the PCF and increase in the duration of the first detached-off Raman soliton, which carries the main part of the output power. As in the previous case, the power of the second Raman soliton in s-polarisation exceeds its power in p-polarisation (Fig. 6, the third row). These features can be explained by the nonlinear polarisation evolution of the pump pulse during its propagation in the PCF. Nonlinear rotation leads to a significant difference of the pump pulse polarisation at the moments of splitting off the first and the second Raman solitons. When the elliptical polarisation becomes close to circular the power of the p-component carrying the most part of the pulse energy decreases. It leads to delay in the pump pulse splitting and suppression of the second Raman soliton by the long-pass filter. The presence of the second Raman soliton can be noted only by small amplitude modulations. In the case of the circularly polarised initial pulse (Fig. 6, the top row), one can see the convergence of the s- and p-components power, however, their complete alignment does not occur. In an ideal isotropic fibre, the circular polarisation of the propagating pulse should be conserved [24]. We can explain this deviation by the possible small PCF twisting.

4. Conclusion

We consider a fibre laser system consisting of a telecom source, a

CPA system, and low-birefringence output LMA PCF. It is shown that the fibre CPA system with average output power of about 300 mW is sufficient to obtain ~ 100 fs pulse of 10.4 nJ energy with central wavelength tunable in the range of 1600–1700 nm by changing the power launched into the PCF. Through experiments, the power, spectral and polarisation characteristics of the Raman soliton spectrum at the PCF output were studied for linear, elliptical and circular input pump pulse polarisations. In case of the circularly polarised initial pulse, the pulse peak power decreases due to the polarisation energy separation. Therefore, the Raman soliton shift in this case is less than for linearly polarised input pulse of the same energy. We have shown that the central wavelength of the output spectrum corresponding to the wavelength of the first Raman soliton can be tuned in the whole range of 1600–1700 nm by adjusting the polarisation state of the pump pulse while the output power remains constant. These properties are extremely attractive for the development of systems for multiphoton imaging of biological tissues.

CRediT authorship contribution statement

D. Stoliarov: Investigation, Data curation, Formal analysis, Validation, Methodology, Software, Writing – original draft. **A. Koviarov:** Investigation, Validation, Methodology. **D. Korobko:** Conceptualization, Methodology. **D. Galiakhmetova:** Investigation, Validation. **E. Rafailov:** Supervision, Writing – original draft.

Declaration of Competing Interest

The authors declare that they have no known competing financial interests or personal relationships that could have appeared to influence the work reported in this paper.

Acknowledgement

DK acknowledges support of the Russian Ministry of Higher Education and Science (project 075-15-2021-581).

References

[1] S.V. Firstov, et al., Bismuth-doped optical fibers and fiber lasers for a spectral region of 1600–1800 nm, Optics letters 39 (24) (2014) 6927–6930.
[2] V.A.G. Rivera, et al., Expanding broadband emission in the near-IR via energy transfer between Er3+–Tm3+ co-doped tellurite-glasses, Journal of Luminescence 145 (2014) 787–792.
[3] L.A. Sordillo, et al., Third therapeutic spectral window for deep tissue imaging, Photonics West - Biomedical Optics (2014).
[4] E. Hemmer, et al., Exploiting the biological windows: current perspectives on fluorescent bioprobes emitting above 1000 nm, Nanoscale horizons 1 (3) (2016) 168–184.
[5] F. Xia, et al., In vivo label-free confocal imaging of the deep mouse brain with long-wavelength illumination, Biomedical optics express 9 (12) (2018) 6545–6555.
[6] L.A. Sordillo, et al., Deep optical imaging of tissue using the second and third near-infrared spectral windows, Journal of Biomedical Optics 19 (2014).
[7] I.A. Bufetov, E.M. Dianov, Bi-doped fiber lasers, Laser physics letters 6 (7) (2009).
[8] T. Noronen, O. Okhotnikov, R. Gumenyuk, Electronically tunable thulium-holmium mode-locked fiber laser for the 1700–1800 nm wavelength band, Optics express 24 (13) (2016).
[9] N.K. Thipparapu, et al., "Bi-doped fiber amplifiers and lasers, " Optical Materials Express 9 (6) (2019).
[10] J.M. Dudley, J.R. Taylor (Eds.), Supercontinuum Generation in Optical Fibers, Cambridge University Press, 2010.
[11] J.P. Gordon, Theory of the soliton self-frequency shift, Optics letters 11 (10) (1986) 662–664.
[12] D.A. Chestnut, J.R. Taylor, Soliton self-frequency shift in highly nonlinear fiber with extension by external Raman pumping, Optics letters 28 (24) (2003) 2512–2514.
[13] D.A. Korobko, et al., Generation of 2 μm radiation due to single-mode fibers with longitudinally varying diameter, Optical Fiber Technology (2019).
[14] J.H. Lee, et al., Soliton Self-Frequency Shift: Experimental Demonstrations and Applications, IEEE Journal of Selected Topics in Quantum Electronics 14 (2008) 713–723.
[15] K.e. Wang, et al., Advanced Fiber Soliton Sources for Nonlinear Deep Tissue Imaging in Biophotonics, IEEE Journal of Selected Topics in Quantum Electronics 20 (2014) 50–60.
[16] J. Santhanam, G.P. Agrawal, Raman-induced spectral shifts in optical fibers: general theory based on the moment method, Optics Communications 222 (2003) 413–420.
[17] T.N. Nguyen, et al., High Power Soliton Self-Frequency Shift With Improved Flatness Ranging From 1.6 to 1.78 μm, IEEE Photonics Technology Letters 25 (2013) 1893–1896.
[18] M. Kato, Wavelength-tunable multicolor Raman soliton generation using an ellipse polarized pump pulse and highly birefringent optical fibers, Journal of Lightwave Technology 24 (2006) 805–809.
[19] N. Nishizawa, et al., Simultaneous generation of wavelength tunable two-colored femtosecond soliton pulses using optical fibers, IEEE Photonics Technology Letters 11 (1999) 421–423.
[20] P. Balla, G.P. Agrawal, Vector solitons and dispersive waves in birefringent optical fibers, Journal of the Optical Society of America B (2018).
[21] Y.u. Du, et al., Self-referenced axial chromatic dispersion measurement in multiphoton microscopy through 2-color third-harmonic generation imaging, Journal of Biophotonics 11 (2018).
[22] Q. Chao, K.H. Wagner, Polarization instability of Raman solitons ejected during supercontinuum generation, Optics express 23 (26) (2015) 33691–33704.
[23] Y. Barad, Y.R. Silberberg, Rotating Solitons in an Isotropic Optical Fiber, QELS 1997 (1997).
[24] S. Tong, et al., Elliptically-Polarized Soliton Self-Frequency Shift in Isotropic Optical Fiber, Journal of Lightwave Technology 39 (2021) 1334–1339.
[25] Redlich, Michael J. et al. "High-pulse-energy multiphoton imaging of neurons and oligodendrocytes in deep murine brain with a fiber laser." Scientific Reports 11 (2021): n. pag.
[26] I.O. Zolotovskii, et al., Generation of a broad IR spectrum and N-soliton compression in a longitudinally inhomogeneous dispersion-shifted fibre, Quantum Electronics 45 (2015) 844–852.